MINERALOGICAL MAGAZINE, DECEMBER 1986, VOL. 50, PP. 567–82

Some geochemical constraints upon models for the crystallization of the upper critical zone–main zone interval, northwestern Bushveld complex

H. V. EALES, J. S. MARSH, A. A. MITCHELL, W. J. DE KLERK, F. J. KRUGER, AND M. FIELD

Department of Geology, Rhodes University, Grahamstown, South Africa

ABSTRACT. Ratios between elements Mg, Fe, Co, Cr, Ni, V, and Sc are consistently different in mafic rocks of the upper critical zone, and those above the Bastard unit. Within the 300 m section above the Merensky Reef, $^{87}Sr/^{86}Sr$ ratios increase from *c.*0.7063 to *c.*0.7087, irrespective of rock type. Decoupling of $Mg/(Mg+Fe^{2+})$ ratios and the Ca contents of plagioclase, and wide variations in the proportions of anorthosite within the Bastard, Merensky, and Merensky Footwall units, are inconsistent with anorthosite formation by simple fractional crystallization of magma batches of limited volume. Conversely, significant differences in Sr-isotope ratios show that these anorthosites could not have shared a common parental liquid. These data are used to develop a model whereby (*a*) the 300 m column above the critical zone represents the mixing of liquids of isotopically and geochemically discrete upper critical and main zone lineages, (*b*) mafic layers of the Bastard, Merensky, and Merensky Footwall units crystallized from discrete injections of primitive, mafic liquid while (*c*) the leucocratic upper parts of these units crystallized during progressive hybridization of liquid residua, which remained after significant separation of mafic phases, with a supernatant column representing the liquid residua of earlier cycles, and (*d*) the buoyancy of plagioclase, and enlargement of the primary phase volume of plagioclase consequent upon an increase in An/Ab ratio of hybrid liquids, were significant factors in the generation of anorthositic layers.

KEYWORDS: layered complex, geochemistry, crystallization, Bushveld complex, South Africa.

MODELS for the origin of layered complexes are, at the present time, more diverse than they have ever been. The preoccupation with fractional crystallization processes that characterized earlier decades has more recently given way to greater emphasis on the behaviour of liquids, and the concepts of stratified liquid columns, double diffusive convection and liquid mixing have done much to introduce greater flexibility in petrogenetic modelling.

However persuasive a genetic model might be, it must satisfy the constraints of hard data. The present paper attempts to establish some such broad constraints, based on six years of field and laboratory studies focused on the north-western limb of the Bushveld complex, and extends and modifies some of our previously published work on limited sections of the complex (Kruger and Marsh, 1982, 1985). The synthesis and sequence of events we adopt here have evolved essentially in compliance with these geochemical constraints; physical aspects dependent on liquid densities, fluid mixing, and crystal fractionation are cursorily treated and constitute the substance of a separate paper. Our data file currently includes *c.*700 new whole-rock analyses for major and trace elements, and *c.*4000 microprobe analyses. Details of analytical procedures are not given here, adequate summaries of our XRF and microprobe methods being given in Eales *et al.* (1980) and Marsh and Eales (1984). Readers are referred to Vermaak (1976) or Coetzer *et al.* (1981) for locality maps and details of the succession at Rustenburg Platinum Mines, Union Section, and to von Gruenewaldt *et al.* (1985) for a review of recent work on the complex.

The present synthesis embodies many of the concepts developed, *inter alia*, by Vermaak (1976), McBirney and Noyes (1979), Campbell *et al.* (1983), Irvine *et al.* (1983), Sparks and Huppert (1984), and Sharpe (1985), to which authors deferential acknowledgement is made.

Cyclic units at R.P.M. Union Section

In any orderly sequence of layers ABCABCABCA, a cyclic repetition is apparent, but the identity of that layer which starts a cycle is not necessarily obvious (cycles might be ABC, BCA, or CAB). Cycles will, however, be unequivocally defined by either (*a*) some parameter that is constant in each cycle, but different in value in successive cycles (fig. 1*a*), or (*b*) a parameter that evolves progressively from some primitive initial value in each cycle, displaying a saw-tooth pattern through the succession (fig. 1*b*).

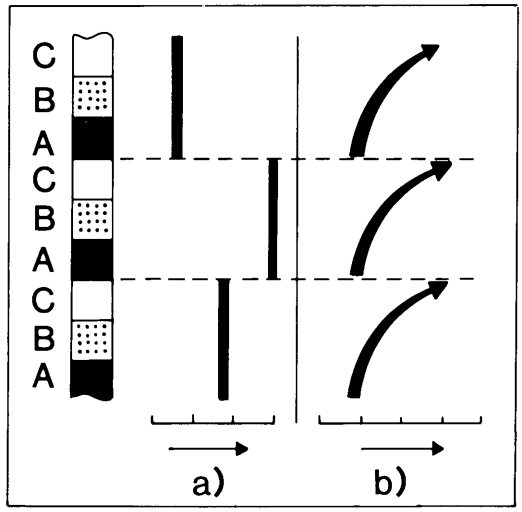

FIG. 1. Schematic representation of geochemical parameters that (*a*) are distinctive of individual cyclic units or (*b*) evolve progressively from some primitive value within each cycle.

The uppermost part of the critical zone of the Bushveld complex displays three particularly well-developed cyclic units, the Merensky Footwall, Merensky, and Bastard units (see stratigraphic column, fig. 2). Vermaak (1976, p. 1277) refers to the latter two as the 'most complete macrocyclic units within the complex'. They exhibit a gradation from chromite- and olivine-bearing rocks at the base, through pyroxenites, melanorites, norites, and leuconorites, to anorthosites at the top. Representative chemical data are given in Table I, and the gradations from one variety to another are depicted by the data of fig. 3. The UG1 and UG2 units (fig. 2) terminate in pyroxenite at Union Section, and thus fail to exhibit the complete sequence through to leuconorite and anorthosite as, for example, in the eastern Bushveld (Gain, 1985). The UG1 Footwall unit is capped by anorthosite at Union Section.

A study by de Klerk (1982) of continuous borehole cores spanning the UG1–Bastard interval at Union Section had previously indicated distinctive ranges in the Sr content of feldspars of the separate cyclic units. These data have now been independently confirmed, and are presented here in fig. 2 in the form of $Sr/Al_2O_3^*$ ratios plotted against stratigraphic height. Although Al is held largely within feldspar, a correction for the small amount in pyroxenes is necessary. The formula:

$$Al_2O_3^* = Al_2O_{3\,rock} - \left(\frac{\text{Mgo in rock}}{\text{MgO in pyroxene}} \times Al_2O_3 \text{ in pyroxene}\right)$$

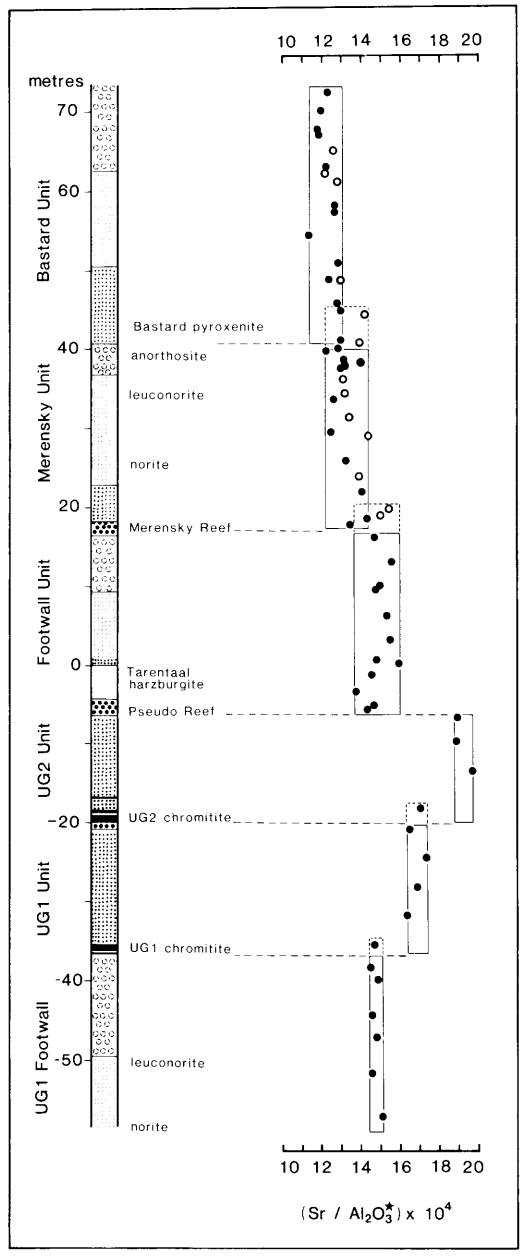

FIG. 2. Stratigraphic column and plot of $Sr/Al_2O_3^*$ ratios *vs.* stratigraphic height at Union Section (filled circles). Methods of calculation are given in text. Open circles depict Sr/Al_2O_3 ratios of plagioclase separates from Rustenburg Section analysed by Kruger (1983). Broken-line boxes represent infiltration of intercumulus liquid into base of unit, from underlying unit.

may be used where samples are, effectively, composed of varying proportions of orthopyroxene and

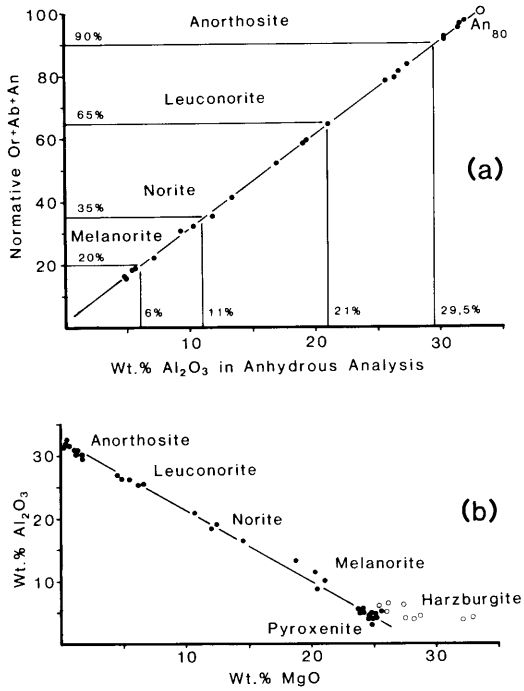

FIG. 3. (*a*) Nomenclature employed for rocks gradational between feldspathic pyroxenite ($< 6\%$ Al_2O_3) and anorthosite ($> 29.5\%$ Al_2O_3). (*b*) Linear variation of anorthosite–feldspathic pyroxenite series on a plot of Al_2O_3 *vs.* MgO (filled circles) and separate field for harzburgites (unfilled circles).

plagioclase (bronzitites, norites, and anorthosites). The entry of olivine as a third phase affects the linear relationship between Al_2O_3 and MgO (fig. 3*b*) and a further correction is required for this (fig. 4). The entry of further phases (mica and chromite, or abundant clinopyroxene) with appreciable levels of Sr and/or Al cannot effectively be corrected for, but such samples are easily identified in thin section and are excluded for present purposes.

A consistent pattern emerges in fig. 2. Successive vertical segments through the column correspond with cyclic units and exhibit distinctive ranges of $Sr/Al_2O_3^*$ values, with steps between the segments. The pattern is that of fig. 1*a*; anorthosites of the Bastard, Merensky, Merensky Footwall, and UG1 Footwall units are geochemically coherent with the underlying more mafic members of the same unit. Additional data pertaining to Rustenberg Section, 70 km to the south, have been incorporated in fig. 2 (open circles) and match precisely the data for Union Section. These data are drawn from Kruger's (1983) analyses of separated mineral fractions which show the average Sr content of plagioclase to be 403 ± 11 ppm in the Bastard unit, 437 ± 18 ppm in the Merensky unit, and 476 ± 18 ppm in the Merensky Footwall unit. Respective averages for Sr/Al_2O_3 in plagioclase are 12.80, 13.88, and 15.04 ($\times 10^{-4}$). It is noted that within the segments (e.g. Merensky and Bastard units, fig. 2) a decline in $Sr/Al_2O_3^*$ ratios with height produces subsidiary trends and broadens the width of segments. This is largely a function of increase in An content (increase in Al) of plagioclase with height in these cycles. A point of interest is that the basal samples of the Bastard, Merensky, UG2 and UG1 units display $Sr/Al_2O_3^*$ ratios more typical of their respective underlying units, suggestive of upward infiltration, through some 3 m, of interstitial, feldspathic residua expelled from below.

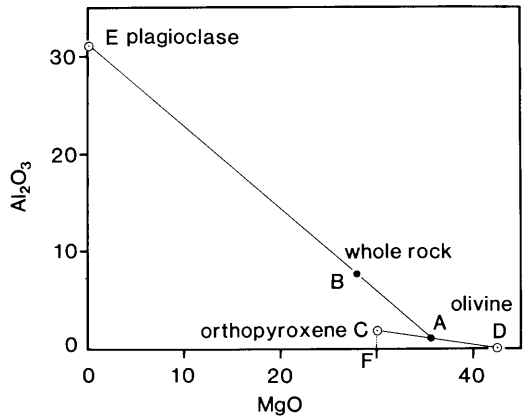

FIG. 4. Procedure for calculating $Al_2O_3^*$ in rocks bearing olivine. Here, $Al_2O_3^* = Al_2O_{3\,rock} - [(AD/CD) \times CF \times (BE/AE)]$ where parameters are taken from whole-rock and microprobe data.

While absolute levels of major and trace elements in quenched liquids or fine-grained rocks can usefully be applied to distinguish rocks crystallized from discrete magma batches (as in Marsh and Eales, 1984), or successive derivative liquids, the dominance of the modal effect inhibits this approach in layered sequences. Virtually any element will show progressive increase or decrease in the sequence peridotite–bronzitite–norite–anorthosite, and yield a saw-tooth pattern through successive cycles, but this is modally controlled and does not, *per se*, define the base of a cycle. Ratios of elements

TABLE I. - REPRESENTATIVE ANALYTICAL DATA

	1	2	3	4	5	6	7	8	9	10	11	12	13	14	15	16	17	18	19	20
SiO_2	48.72	48.46	47.97	49.56	49.95	50.31	50.64	51.39	53.11	52.87	52.35	53.07	44.98	40.74	51.75	51.74	51.74	51.49	51.33	51.79
TiO_2	0.00	0.08	0.06	0.17	0.12	0.11	0.12	0.13	0.22	0.25	0.20	0.23	0.16	0.09	0.12	0.12	0.15	0.16	0.13	0.15
Al_2O_3	32.09	30.90	31.00	28.61	23.70	19.70	16.81	10.98	5.32	4.76	4.75	4.09	5.42	4.66	22.26	19.16	17.81	18.15	27.69	19.14
Fe_2O_3	1.04	1.91	2.06	2.56	4.57	5.92	7.10	9.16	12.09	12.28	12.29	13.10	16.80	15.48	5.00	6.58	6.00	6.56	2.39	5.89
MnO	0.01	0.01	0.01	0.04	0.07	0.09	0.13	0.15	0.19	0.21	0.21	0.26	0.21	0.17	0.07	0.10	0.11	0.11	0.02	0.12
MgO	0.72	1.04	1.38	2.64	7.59	11.87	14.70	20.73	24.20	24.82	25.11	25.00	28.80	35.76	6.65	9.32	9.20	9.33	1.98	7.65
CaO	15.11	15.08	14.82	14.16	12.14	10.25	8.96	6.34	3.86	3.92	4.10	3.38	3.04	2.71	11.66	10.67	12.91	12.19	13.28	12.96
Na_2O	2.16	2.35	2.39	2.00	1.65	1.55	1.32	1.06	0.85	0.81	0.77	0.63	0.50	0.33	2.23	2.13	1.91	1.82	2.66	2.11
K_2O	0.12	0.15	0.31	0.24	0.19	0.18	0.23	0.06	0.16	0.09	0.12	0.22	0.10	0.06	0.25	0.17	0.16	0.17	0.52	0.21
P_2O_5	0.03	0.03	n.d.	0.03	0.02	0.02	n.d.	n.d.	tr.	tr.	0.02	0.03	tr.	tr.	tr.	0.01	tr.	0.01	tr.	0.01
Rb	1.7	3.0	11	5.8	4.7	1.7	3.1	n.d.	6.9	4.0	5.7	7.1	3.5	3.0	4.1	n.d.	3.2	3.2	7.9	4.0
Sr	466	460	396	341	276	237	183	125	56	52	68	44	70	61	288	262	232	221	336	256
Y	n.d.	3.0	2.3	n.d.	n.d.	3.0	4.0	3.7	7.2	7.5	8.4	7.7	3.8	3.0	5.2	5.2	6.5	7.7	5.3	6.6
Zr	n.d.	7.8	5.7	n.d.	n.d.	6.5	5.0	4.5	24	21	16	15	10.3	6.0	12.9	4.6	7.1	10.7	19.4	12.3
Ba	54	64	87	n.d.	n.d.	43	43	25	67	45	49	55	31	25	92	77	70	74	116	83
Sc	3.3	8.0	7.0	6.5	11	16	22	26	34	34	34	36	13	11	13	17	23	23	11	23
V	11	17	16	38	55	63	72	95	113	137	131	153	67	36	75	90	129	122	42	112
Cr	47	63	161	176	851	1400	1795	2630	2960	2850	3380	3735	3820	1405	351	405	530	454	42	105
Co	7.1	8.2	8.8	17	35	51	57	76	99	104	92	104	170	132	36	42	44	51	15	42
Ni	13	24	84	50	161	281	316	369	774	1165	582	650	1855	1750	153	174	207	228	37	158
Cu	10	27	54	16	19	18	19	14	170	370	42	24	400	19	19	18	18	27	13	19
Zn	7.0	9.3	9.0	17	32	40	41	54	82	77	79	83	70	61	35	37	43	54	18	33

1. Anorthosite : UG1 Footwall unit (3 samples).
2. Anorthosite : Merensky Footwall unit (3 samples).
3. Anorthosite : Merensky unit (3 samples).
4. Anorthosite : Bastard unit (3 samples).
5. Leuconorite : Bastard unit.
6. Norite : Bastard unit (2 samples)
7. Norite : Bastard unit.
8. Melanorite : Bastard unit (2 samples).
9. Pyroxenite : Bastard unit (2 samples).
10. Pyroxenite : Merensky unit.
11. Pyroxenite : UG2 unit (3 samples).
12. Pyroxenite : UG1 unit (5 samples).
13. Merensky Reef (2 samples).
14. Tarentaal harzburgite, Merensky Footwall unit (2 samples).
15. Average leuconorite, 100-235 m above Bastard Reef (3 samples).
16. Average leuconorite, 235-330 m above Bastard Reef (major elements : 2 samples; trace elements : 12 samples).
17. Porphyritic Gabbro Marker, 340-400 m above Bastard Reef (3 samples).
18. Gabbro, 407-533 m above Bastard Reef (major elements : 3 samples; trace elements : 11 samples).
19. Leucogabbro, 581-595 m above Bastard Reef (major elements : 3 samples; trace elements : 6 samples).
20. Gabbro, 700-880 m above Bastard Reef (major elements : 4 samples; trace elements : 11 samples).

n.d. Below limit of determination, or data not available.

tr. Less than 0.01%. Major-element analyses normalised to 100% L.O.I.-free, and trace elements in ppm (without normalization). All Fe is given as Fe_2O_3.

selected on a basis of their occurrence in one phase and virtual exclusion from others should, however, be independent of modal proportions (e.g. the ratios of two elements within orthopyroxene should remain the same irrespective of whether 20 or 60% of orthopyroxene exists in the rock). Should the ratio show progressive change from some primitive value through a sequence of rocks, this would constitute evidence for consanguinity of the sequence. A geochemical discontinuity would indicate a lithological hiatus. This principle is investigated in fig. 5.

Fig. 5 illustrates various ratios plotted against stratigraphic height within the UG1 Footwall, Merensky Footwall, Merensky, and Bastard units. Olivine-bearing rocks are excluded. Within the Merensky unit, MgO/(MgO + FeO) ratios show little variation below a threshold whole-rock value of 26% Al_2O_3 but rapid decline in the ratio occurs within the overlying leuconorites and anorthosites. A minor reversal in trend occurs in the uppermost sample, immediately beneath the Bastard Reef. Co/V, Ni/Sc, Cr/Sc, and Cr/V ratios decline more or less steadily through the unit, apart from a minor reversal which again appears at the top of the unit. Trends within the Bastard and Merensky Footwall units are broadly similar, but distinct inflections occur between the mottled anorthosites and leuconorites (so-called spotted anorthosites), consistent with the field evidence of a mappable basal contact to mottled anorthosite. These trends cannot be discounted by recourse to arguments that they merely depict modal variations—that Cr/V ratios are, for example, controlled by accessory chromite. The Merensky and Bastard unit feldspathic pyroxenites represented contain no more than trace amounts of chromite, and whole-rock levels of Cr in them (2600–2850 ppm) are appropriate to the levels of Cr (2400–3700 ppm) measured in pyroxene separates by Kruger (1983). Furthermore, Cr/V

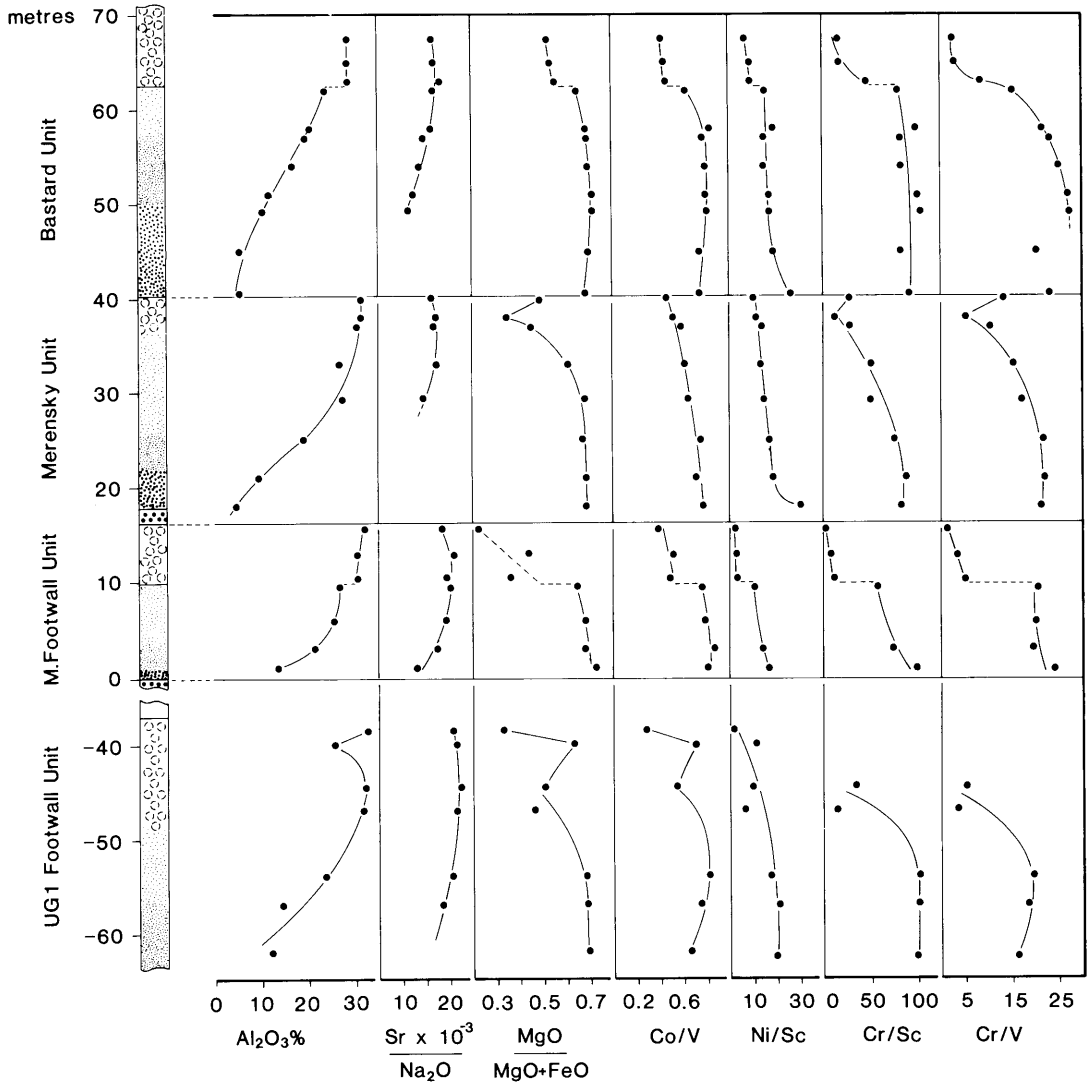

FIG. 5. Whole-rock Al_2O_3 levels and inter-element ratios within four cyclic units of the upper critical zone. Harzburgites and rocks containing chromite are exluded.

ratios in such separates range from 21–27, at the base of the Merensky and Bastard units, to *c.*5 at their tops, matching the whole-rock data of fig. 5.

The significance of fig. 5 lies in the evidence that there is no geochemical discontinuity between anorthosite with > 30% Al_2O_3, and the underlying more mafic rocks in the Merensky unit, or between leuconorite (24–27% Al_2O_3) and more mafic rocks of the Bastard and Merensky Footwall units. Furthermore, although each unit is capped by anorthosite, these felsic layers are geochemically dissimilar with respect to both major- and trace-element composition, in the separate cycles. There is no evidence to support a common parent liquid for all the anorthosites. Sparse geochemical data for the anorthosites of the UG1 Footwall unit (fig. 5) reflect similar relationships, although considerable scatter in the data shows the transition to felsic rocks at the top of the unit to be more irregular than in the other cycles above it. We conclude therefore

that mafic cumulates constitute the base, and anorthositic rocks the top, of cyclic units.

Sections compiled by Vermaak (1976), and his original data (pers. comm.), show that the proportion of leuconorite plus anorthosite within the Merensky unit varies from as little as 33% to as much as 85% in various sectors of the complex. It is inconceivable that such wide variations in total feldspar could attend the crystallization of a single injection of homogeneous parental liquid. Accordingly, either substantial losses or gains of feldspar must have accompanied the development of the Merensky unit. The same conclusion would appear feasible to account for the different proportions of feldspar in the Bastard, Merensky, and Merensky Footwall units.

These observations are relevant in the context of some current models for layered complexes, proposing that cyclic units are the result of a mixing of liquids. Keith *et al.* (1982) and Irvine *et al.* (1983) define several major zones in the Stillwater complex in terms of cyclic units passing upwards through anorthosite–peridotite–troctolite–pyroxenite–norite. This model is extrapolated by them to explain the Bushveld complex as well. Critical to the thesis of Irvine, Keith and coworkers is the injection of dense, relatively cool, anorthositic (A-type) liquid beneath liquid derivatives of a less dense, but hotter picritic (U-type) melt. Hybridization leading to olivine-saturated melts is proposed, with 'finger-type' mixing and convergence of liquid densities in the earlier stages; with heating of the lower A-type derivative, and heat loss from the overlying U-type derivatives, a series of stabilized diffusional interfaces evolves with time. Crystallization from this system, they propose, leads to the sequence anorthosite–peridotite–(troctolite)–bronzitite–norite. Abrupt lithological transitions of this sort, between peridotitic rock (above) and anorthosite (below) are well established in the upper critical zone, but they are not uniquely explained by this or any of several alternative models. The Irvine–Keith model is unique, however, in requiring the A-type derivative liquids, resting upon the previous floor of the intrusion, to deposit rocks of the anorthositic lineage upon that floor, which, in principle, could be any member of the picritic lineage. Any geochemical differences between A-type and U-type liquids should then be manifest across the contact between anorthosite and its footwall. Geochemical consanguinity ought not to be displayed between anorthosite and norite, particularly with respect to trace element data. Furthermore, the anorthosites within successive cyclic units should be geochemically similar, if not identical, if (as in Irvine *et al.*, 1983, p. 1317) they are deposited from a common parent liquid as it is lifted or dropped to different levels by events within the chamber. We find, in the data summarized in fig. 5, that there are distinct geochemical differences between the anorthosites of the separate units, and that there is no geochemical discontinuity in the norite–leuconorite–anorthosite sequences of the Merensky and UG1 Footwall units, i.e. no obvious break in trends as whole-rock Al_2O_3 levels rise from $< 10\%$ to $> 30\%$. In the case of the Bastard and Merensky Footwall units, inflections are evident, respectively, between rocks with 23·5% and 28·5% Al_2O_3, and 26·5% and 30·5% Al_2O_3. The proposition that these inflections might mark the emplacement of A-type liquids above a floor derived from the U-type lineage is difficult to accept. Sharpe's (1985) putative U-type lineage displays consistently high Zr/Y ratios (*c.*6–8) and the A-type lineage low ratios (*c.*1.2–4.5). None of the cyclic units of fig. 5 shows any trend towards decreasing Zr/Y between pyroxenitic and anorthositic layers.

The critical zone–main zone transition

In the Union Section area, some 3 km of main zone rocks overlie the critical zone. The spectacular layering and lithological diversity of the critical zone give way to a more uniform succession of norites and gabbronorites, their leucocratic variants, and anorthosites. Chromitite, harzburgite, and olivine-bearing rocks are absent, and pyroxenite is rare. Modal analysis of seventy-five samples through the lowermost 2.8 km at Union Section (Mitchell, 1986) shows that $> 80\%$ of rocks contain 50–80% plagioclase feldspar; orthopyroxene and clinopyroxene are generally present in a ratio of *c.*2 : 1. A broad subdivision into subzones A, B, and C is used. Subzone A comprises the lowermost 1 km and, apart from the lowermost 50 m, is characterized by primary orthopyroxene. An important marker is the 'Porphyritic Gabbro Marker' (P.G. Marker of fig. 6). Subzone B is *c.*1.2 km thick and the Ca-poor pyroxene is inverted pigeonite. At the level of the 'Pyroxenite Marker', Subzone B passes into Subzone C. A geochemical change to more primitive compositions, and reappearance of primary orthopyroxene, occurs above the junction.

Previously unpublished data are presented here in figs. 6 and 7, which stress Mg–Fe and transition trace-element relationships, and fig. 8, which stresses chemical features associated with feldspars. Paradoxically, the two sets of data lead to seemingly conflicting interpretations.

Chemical data relating to mafic phases. The whole-rock ratios MgO/(Mg + FeO), Cr/Co, Co/V, and Ni/Sc of main zone rocks and the more mafic

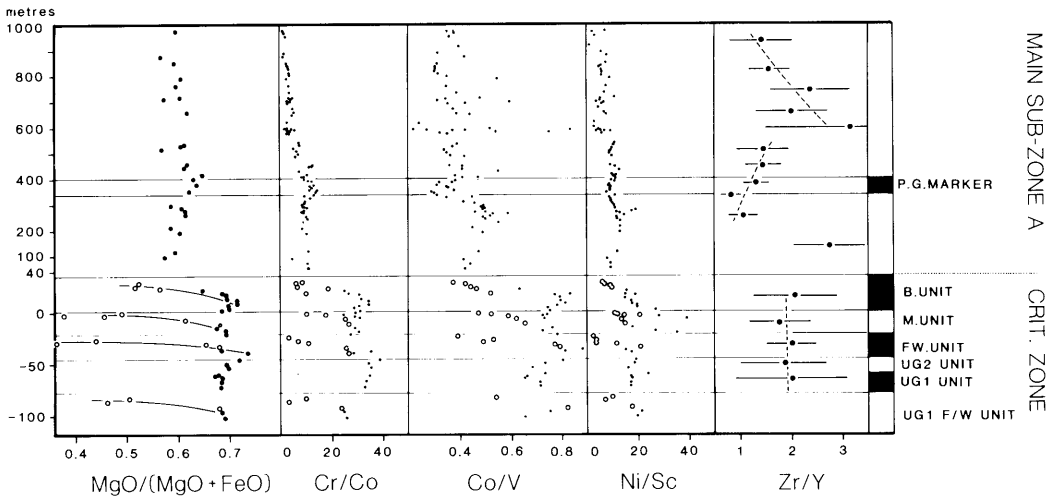

FIG. 6. Diagram illustrating geochemical differences between mafic rocks of main and upper critical zones (filled circles). Leucocratic rocks of critical zone are depicted by unfilled circles. Note scale change between 40 and 100 m. Porphyritic Gabbro Marker is shown between 340 and 400 m.

rocks of the upper critical zone (filled circles of fig. 6) display an abrupt change of values above the Bastard unit, with virtually no overlap in the data sub-sets from above and below the contact. No convergence is displayed as the contact is approached. Co/V ratios (apart from an anomalous horizon at 580 m height, fig. 6) are consistently $< 0{\cdot}55$ above the junction, and 0.66–0.88 below it. Cr/Co ratios are between 1 and 14 above, and 25–40 below the junction. Mg/Fe ratios actually diverge most widely closest to the junction. The increase in Mg-number with increasing stratigraphic height within the first 340 m above the Bastard unit has been further substantiated by detailed microprobe studies of ortho- and clinopyroxenes (Mitchell, 1986). In detail, the increase is not regular, but follows a saw-tooth pattern not evident in the more sparse data points of fig. 6.

The abrupt transition above the Bastard unit is further emphasized by the data of fig. 7, depicting Cr/Al ratios of orthopyroxenes. A simplified representation of orthopyroxene is $(Mg,Fe)SiO_3$, but the entry of trivalent cations is effected by a Tschermak-type substitution, yielding $(Mg,Fe,Al,Cr)(Si,Al)O_3$. While rather wide ranges in absolute levels of Al and Cr may exist, Cr/Al ratios show restrained variations in geochemically coherent suites (Eales and Marsh, 1983). Fig. 7 summarizes currently available data based on microprobe studies of the main zone (Mitchell, 1986) and the upper critical zone (de Klerk, 1982; and unpublished data of H.V.E.) at Union Section, and the lower critical and lower zones in the Eastern Transvaal (Cameron, 1980, 1982, and extensive unpublished data). Despite obvious objections to combining data from eastern and western sectors, the good match of Cameron's data for the lower critical zone and our data for the upper critical zone suggests that the plot is valid. An abrupt geochemical break is apparent at the top of the Bastard unit. Further breaks occur at 530–580 m above the Bastard unit, and at the Pyroxenite Marker (*c.*2240 m) above which there is a reversion to ratios found within the lowermost 500 m of main subzone A.

It is difficult, in the light of figs. 6 and 7, to sustain a simple model of mixing of main zone liquids with critical zone liquids within subzone A, to yield a hybrid sequence that included the Merensky and Bastard units at its base, as advocated by Sharpe (1985). Progressive mixing of A-type liquids with U-type liquids, exhibiting the compositional attributes specified by Harmer and Sharpe (1985) and Sharpe (1985), would inevitably have yielded intermediate ranges of MgO/(MgO+FeO), Cr/Co, Co/V, and Ni/Sc ratios where they mixed. The Merensky and Bastard units would have been members of such an intermediate suite. The trends we find do not depict this.

In fig. 6 the more mafic rocks of the upper critical zone (filled circles) have been distinguished from the more felsic varieties (unfilled circles) constituting the upper parts of the cyclic units. A cut-off value of 310 ppm Sr (*c.*22% Al_2O_3) has been used. It is clear that the *felsic* members of the UG1 Footwall, Merensky Footwall, Merensky, and Bastard units display compatible element ratios that converge

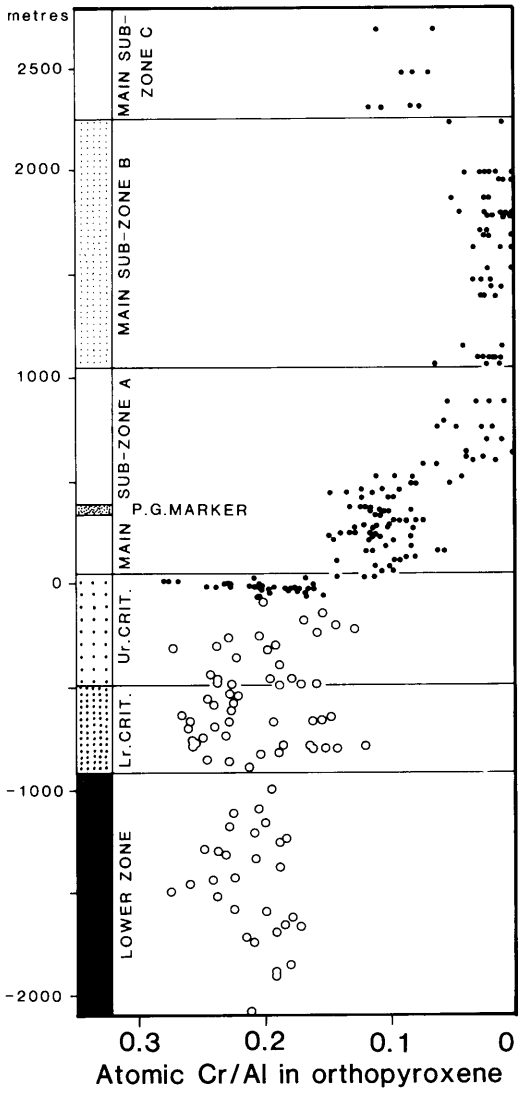

FIG. 7. Atomic Cr/Al ratios of orthopyroxenes in lower, critical, and main zones, as determined by microprobe analysis. Data sources are given in text, with Cameron's data being represented by unfilled circles. Boundary between upper critical and main zones is drawn at the top of the Bastard unit; Pyroxenite Marker horizon separates main subzones B and C; Porphyritic Gabbro Marker is shown as P.G. Marker.

with those of the main zone. Whether this is due to hybridization of liquids, or fractionation, is discussed later.

Incompatible elements. Elements Rb, Zr, Y, Nb, and P are present at low levels in most samples (see Table I) and absolute concentrations are somewhat unpredictable. Not only does the analytical accuracy of XRF methods deteriorate at these low levels, but the 'degree of incompatible behaviour' becomes significant. Only two generalizations appear to be broadly applicable. First, incompatible element levels do not rise with height within individual cyclic units. Data from Rustenburg (Kruger, 1983), Union (de Klerk, 1982), and Amandelbult (Scoon, 1985) Sections are consistent in showing that, in the Merensky unit, levels of these elements tend to be highest in the basal layers. Kruger's data show Zr contents of the Merensky anorthosite to be 2.6–5.7 ppm, leuconorites and norites 2.9–7.3 ppm, the Merensky pyroxenite *c.*22 ppm, and the basal, olivine-bearing Merensky pegmatoid 12–26 ppm. Respective values for Rb are 1.7–3.2, 1.4–2.9, 4.9, and 3.8–9.7 ppm and for Y 2.2–3.1, 1.8–5.2, 10.2, and 4.6–16.6. Considering that the basal pegmatite and pyroxenite consist largely of ferromagnesian phases, actual levels of incompatible elements in intercumulus space must be appreciably higher.

A second generalization is illustrated in fig. 6. Zr/Y ratios appear to separate the upper critical zone, the 340–570 m interval, and the interval above 600 m into discrete lineages.

Chemical data relating to the feldspars. Whole-rock data which are largely a function of feldspar chemistry are presented in fig. 8. The available Sr-isotope data have been compiled from the work of Kruger and Marsh (1982), Kruger (1983), and Kruger and Mitchell (1985). These isotope ratios are sensibly constant at 0.7063 in the Merensky Footwall unit, but rise rapidly through and above the Merensky pyroxenite. This increase is sustained through the Bastard unit and the first 350 m in the main zone, with a levelling-out in the vicinity of the Porphyritic Gabbro Marker. The increase in isotope ratios is seemingly unaffected by the extreme modal variations from pyroxenite to anorthosite within the Merensky Footwall, Merensky, and Bastard units. In so far as Sr-isotope ratios are unaffected by crystal fractionation, the trends constitute persuasive evidence in support of some form of mixing between two end members with initial ratios, respectively, of 0.7064 ± 0.0001 and 0.7087 ± 0.0003. High isotope ratios (> 0.708) characterize most of the main zone until the Pyroxenite Marker is reached at 2240 m above the Bastard Reef, at which point other geochemical parameters such as Cr/Al ratios of pyroxenes (fig. 7) and whole-rock data (Mitchell, 1986) revert to values more typical of the base of the main zone. At this same level, Sr-isotope ratios decline rapidly to 0.7077 at 2270 m and 0.7073 at 2600 m above the Bastard Reef (Kruger and Mitchell, 1985).

The systematic increase in Sr-isotope ratios

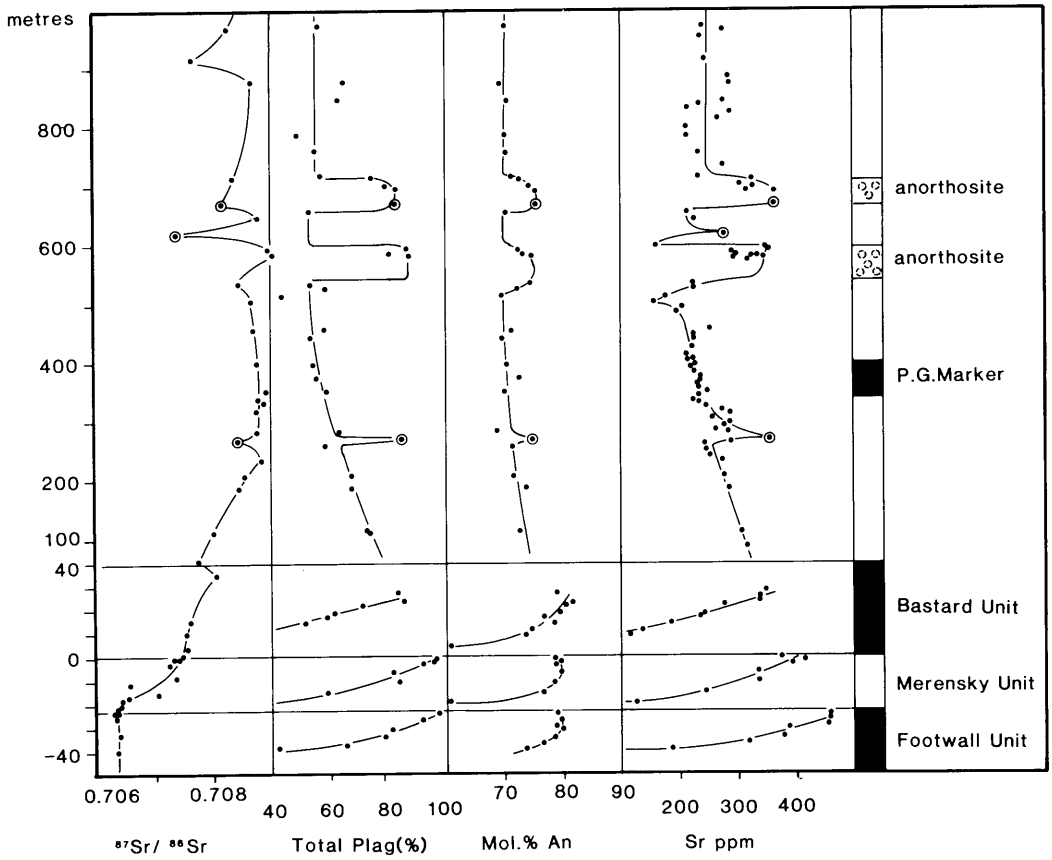

FIG. 8. Whole-rock chemical data dependent on feldspar composition, upper critical and main zones. Note scale change between 40 and 100 m. Ringed circles identify feldspar-rich samples with anomalously low Sr-isotope and elevated An/Ab ratios. Profile of isotope ratios is composite, based on data from Union and Rustenburg Sections.

through the Merensky and Bastard units, irrespective of rock type, strengthens our earlier conclusion that the anorthosites within these cyclic units are not derivatives of a common parent liquid. Furthermore, if these anorthosites were derivatives of an aluminous liquid of the main zone lineage emplaced beneath more mafic derivatives (Irvine *et al.*, 1983) it is difficult to envisage how the steady increase in isotope ratios could have been sustained through the Merensky and Bastard units. A sawtooth trend would be anticipated.

Apart from the broad trends described above, the data reveal that at 270, 620, and 670 m, Sr-isotope ratios are appreciably lower than would be expected from interpolation between adjacent samples. The low values are at 270 and 670 m associated (fig. 8) with local increases in total feldspar content, as monitored by normative data and whole-rock Sr contents, and with increases in the proportion of the calcic component of the plagioclase. At 620 m, the Sr-isotope ratio is the same as that at the top of the Merensky unit.

A further conclusion drawn from the steady increase in isotope ratios above the Merensky Reef is that there is little support for the suggestion of Irvine *et al.* (1983) that the Pseudo, Merensky, and Bastard units are equivalent, representing deposits laid down from the same liquids re-elevated to different levels within the chamber at different times.

Summary of and commentary on the more significant geochemical criteria

1. The UG1 Footwall, UG1, UG2, Merensky Footwall, Merensky, and Bastard units exhibit different narrow ranges of $Sr/Al_2O_3^*$ ratios; this is suggestive of each cycle being representative of a

separate injection of magma. Infiltration of liquid residua from the top of one cyclic unit into intercumulus space in the base of the succeeding unit is not significant beyond *c.*3 m.

2. Anorthosites at the top of the UG1 Footwall, Merensky Footwall, Merensky, and Bastard units display $Sr/Al_2O_3^*$ ratios that match those of their immediately underlying norites and feldspathic pyroxenites.

3. $Sr/Al_2O_3^*$ ratios of anorthosites are $(11.7–12.7) \times 10^{-4}$ within the Bastard unit, $(12.2–13.9) \times 10^{-4}$ within the Merensky unit, $(13.6–15.8) \times 10^{-4}$ within the Merensky Footwall unit and Pseudoreef at its base, and $(14.3–15.1) \times 10^{-4}$ within the UG1 Footwall unit. The anorthositic layers do not, therefore, appear to be derivatives of any single, common liquid, unless this liquid was undergoing continuous contamination. This ratio fluctuates but little $(12.2–14.2) \times 10^{-4}$ within the overlying 1000 m column of main zone rocks.

4. Sr-isotope initial ratios increase from *c.*0.7063 at the top of the Merensky Footwall unit, through 0.7075 at the base of the Bastard unit, to *c.*0.7087 at a level 310 m above the base of the Merensky unit. A value of 0.7087 ± 0.0003 is maintained for the following 300 m. In so far as Sr-isotope ratios cannot be affected by crystal fractionation, a mixing of new liquid (isotope ratio 0.7087 ± 0.0003) with an older liquid (isotope ratio 0.7064 ± 0.0001) through a vertical interval of 300 m is a feasible hypothesis.

5. Within the interval extending from 340 to 570 m above the Bastard unit, rocks that are indicated by Sr-isotope data to represent a homogeneous group are seen to be geochemically coherent with respect also to ratios between the compatible elements (fig. 6). It is considered that this interval represents a sample of cumulates deposited by a new influx of magma, uncontaminated by mixing or hybridization, that was emplaced above liquids overlying critical zone cumulates. This interpretation is developed later in fig. 11.

6. A number of highly feldspathic intervals occur within the first 1200 m of the main zone. Sr-isotope initial ratios vary erratically and within some samples may be substantially depressed within these intervals, relative to values in overlying and underlying gabbronorites. At a level 630 m above the Merensky unit, there occur anorthosites with the same isotope ratios as are typical of the Merensky unit itself. Plagioclase in these anorthosites may be up to 5% more calcic than that in the enclosing gabbronorites and, as such, its composition is closer to that found at the top of the critical zone than it is to that typically occurring at this level within the complex. We consider these intervals to include feldspathic crystal mushes, or schlieren, entangled with or uplifted by influxes of new magma that contributed to the main zone (Eales, in press).

7. Whereas the Sr-isotope data are supportive of a simple model depicting a lower column of rocks (i.e. below the Merensky unit) which is petrologically distinct from an upper column (commencing 340 m above the Bastard unit), with a 350 m zone of mixing intervening between the two, geochemical data relating to Fe, Mg, Cr, Co, V, Ni, and Sc indicate (fig. 6) a much more complex interpretation of the junction between the critical and main zones.

8. Cr/Al ratios of orthopyroxenes, determined by microprobe analysis, are 0.170–0.275 within the lower zone, 0.120–0.275 within the critical zone, 0.045–0.280 within the succeeding 580 m interval, and < 0.075 above this. As with isotope and other whole-rock data (Mitchell, 1986) a sharp break occurs at the top of main subzone B (*c.*2240 m above the Bastard unit) above which Cr/Al values revert to those found immediately above the critical zone. These data would be consistent with a process entailing mixing of Cr-depleted liquid residua from the critical zone with newly emplaced liquids of which cumulate rocks within the 340 to 570 m interval are representative. If so, it follows that the chemically distinct package that comprises the upper half of main subzone A, and the whole of subzone B, represents a further intromittent wedge or series of wedges of magmatic liquids, emplaced beneath main subzone C.

9. Plots of the whole-rock ratios $MgO/(MgO + FeO)$, Cr/Co, Co/V, and Ni/Sc (fig. 6) show that the mafic rocks of the Bastard, Merensky and underlying units exhibit ranges of values that are significantly different to those within the succeeding 1000 m column, with virtually no overlap. An abrupt change in geochemical signature occurs immediately above the Bastard unit. Mafic rocks of the upper critical and main zones thus appear to belong to discrete lineages. Sr-isotope ratios thus indicate a change of lineage commencing at the base of the Merensky unit; compatible element data pertaining to the mafic rocks indicate that the change occurs above the Bastard unit.

10. Each of the Bastard, Merensky, Merensky Footwall, and UG1 Footwall units exhibits a sequence from mafic–ultramafic layers at the base to leuconoritic and anorthositic layers at the top. Concomitantly with the decline in colour index, there is within each cycle a gradation of ratios between compatible elements Mg, Fe, Cr, Co, V, Ni, and Sc towards values that are closer to those found within the overlying main zone succession (fig. 6). The question therefore arises whether such 'com-

plete' cycles owe their origin to (*a*) mixing of mafic, critical zone-type liquids (which yield the basal, mafic cumulates with typical critical zone geochemical signatures) with main zone liquids (which yield the leuconorites and anorthosites, with geochemical signatures akin to main zone rocks) or (*b*) fractional crystallization of discrete liquid layers, or (*c*) some other mechanism.

11. A number of features emphasize the inadequacies of both models (*a*) and (*b*) above. Specific objections to a simple mixing of liquids of the critical and main zone lineages within each cycle are: (i) Sr-isotope ratios are markedly different within the anorthosites of each of the Merensky Footwall, Merensky, and Bastard units, showing that these anorthosites cannot be derivatives of a common parent liquid. Isotope signatures of these anorthosites are in turn also different to those of main zone rocks, (ii) differences in $Sr/Al_2O_3^*$, MgO/(MgO + FeO), Ni/Sc, and Cr/V ratios of these anorthosites, as well as major-element analyses, lead to the same conclusion, and (iii) MgO/(MgO + FeO) ratios may drop to values lower in these anorthosites than those in rocks of the main zone. Specific objections to the derivation of the leucocratic rocks of the cyclic units by simple crystal fractionation of restricted volumes of melt are: (i) the increase in Sr-isotope ratios between bases and tops of the Merensky and Bastard units, (ii) the highly variable proportions of feldspar within these cyclic units, notably within the Merensky unit. The conclusion seems inescapable that either feldspar loss, or feldspar gain, has characterized different exposures of the Merensky unit, (iii) microprobe and whole-rock data (Kruger, 1983; Mitchell, 1986) emphasize that MgO/(MgO + FeO) ratios decline while plagioclase feldspars become calcic, upwards through the Merensky unit. This decoupling of trends is incompatible with simple fractionation, and characterizes both Union and Rustenburg sections. The data of Gain (1985, fig. 4) show the same features in the UG1 and UG2 units at Maandagshoek, and (iv) there are difficulties involved in deriving anchimonomineralic anorthosites by progressive crystallization of mafic liquids (Irvine *et al.*, 1983).

Discussion

A multiplicity of cyclic units has been laid down by crystallization within the lower and critical zones. Irrespective of whether these represent the precipitates from many, or but a few magma inputs, there is abundant evidence for the truncation of units at various stages of growth. Units that terminate in some areas in pyroxenite, continue upwards into more highly feldspathic layers when followed along strike. The conclusion is inescapable that a supernatant column of liquid residua, relatively depleted in ferromagnesian components, must have collected above the crystalline floor, as there is no evidence for contemporary volcanism by which residua could have escaped. Our synthesis argues that cyclic units of the upper critical zone show evidence of interaction between newly emplaced liquids, and these residua.

By virtue of its being a residuum after the separation of olivine, chromite, and bronzite, the supernatant column would be expected to be relatively depleted in Mg, and elements with high bulk distribution coefficients (Cr, Ni, and Co) but to display raised Fe/Mg ratios and enrichment in potential feldspar. Protracted crystallization of anhydrous phases should have elevated its H_2O content above that of the primitive liquids.

Vital to any understanding of the upper critical-lower main zone interval is the origin of the anorthosite layers. As stressed by Irvine *et al.* (1983) conventional trajectories through relevant phase diagrams do not lead from picritic liquids to anorthosite. We stress here also the interpolation of anorthosites within norites (Vermaak, 1976, p. 1287; Kruger, 1983), the highly variable proportions of anorthosite within cyclic units (e.g. the Merensky unit), the not uncommon occurrence of sharply defined basal contacts, their variability in composition and Sr-isotope ratios, and, commonly, feldspars that are more calcic than in associated norites and gabbronorites. The latter attribute is clearly shown within the cyclic units of the upper critical and main zones at Union Section (fig. 8); it is verified by Kruger (1983) and Kruger and Marsh (1985) at Rustenburg Section; and it is evident in Cameron's data (1982, figs. 2–3) for the F, H, and M2 units in the eastern sector, and in Gain's (1985) data for the UG1 and UG2 units. A decoupling of trends of cryptic variation in orthopyroxene and plagioclase feldspar is evident in the data of Cameron (1982), de Klerk (1982), Kruger (1983), and Gain (1985). None of these features appears consistent with the derivation of anorthosites by progressive fractionation alone.

Studies of chromitites in the upper critical zone (Eales, in press; Eales and Reynolds, in press) have helped to shed light on the paragenesis of feldspar in these rocks. The UG1 unit displays a number of thin chromitite layers intercalated with pyroxenites above the thick, basal chromitite layer. Cryptic variations in the form of upward increase of Fe^{3+} and Ti levels, and decline in Al/Cr ratios are evident in the successive chromitite layers. Experimental evidence exists to show that concomitant crystallization of feldspar leads to decline in the latter ratio in spinels. We conclude that in the upper critical

zone chromite initially crystallized together with bronzite, but in the later stages with feldspar as well. The enclosing pyroxenites contain intercumulus plagioclase only, hence it is believed that although bronzite, chromite, and plagioclase have co-precipitated, the modal composition of these rocks did not instantaneously reflect this. We attribute this to convective turbulence within newly emplaced liquid layers, which physically inhibited inclusion of cumulus feldspar within the pyroxenites. The plausibility of this view is enhanced by experimental data which indicate positive buoyancy of feldspar in basaltic melts (Campbell *et al.*, 1978). An important consequence of the floating of early crystallized feldspar would be that the residual intercumulus liquid in the basal layers of cyclic units would evolve to more sodic compositions. Crystallization of this liquid would yield intercumulus feldspar that is less calcic than cumulus feldspar in higher layers. If the development of a cyclic unit were to be terminated by beheading, on injection of a fresh pulse of primitive liquid, reheating would raise the An/Ab ratio within the basal part of the column of supernatant residual liquid, by partial resorption of the suspended feldspar (see fig. 9).

The pronounced changes in major- and trace-element composition between pyroxenites and anorthosites of 'complete' cyclic units are thus here attributed to initial crystallization of mafic phases within a basal layer of newly emplaced primitive liquid, followed by progressive hybridization with the supernatant column of residual liquids. The mafic members of each unit would thereby reflect the compatible-element chemistry of each fresh magma input, but a gradation to the compositional attributes of a more evolved derivative would be displayed within the leucocratic members (see figs. 6 and 8). The trends would simulate fractionation, but arise in part by a mixing process. The mixing would be a consequence of the convergence of liquid densities of the basal liquid layer and the supernatant column. Disintegration of the diffusive interface would follow. The decline in density of the basal layer would be a mandatory result of the separation of olivine, chromite, and bronzite. Addition of plagioclase to the crystallizing assemblage would normally be expected to increase the residual liquid density (Sparks and Huppert, 1984) but this effect would have been inhibited where significant amounts of feldspar were retained in suspension within the liquid, as suggested above.

A further consequence of mixing of the upper, chemically evolved part of the basal, picritic liquid layer with the accumulated residuum above would be an increase in the calcic components of plagioclase in the hybrid liquid produced (fig. 9). The liquidus fields of more highly polymerized silicate structures are increased by decreasing molecular proportions of monovalent cations (Kushiro, 1975), and Irvine (1970, fig. 12) has charted the expansion, with increased An/Ab ratios within the olivine-orthopyroxene-plagioclase-clinopyroxene system, of the primary phase volume of plagioclase.

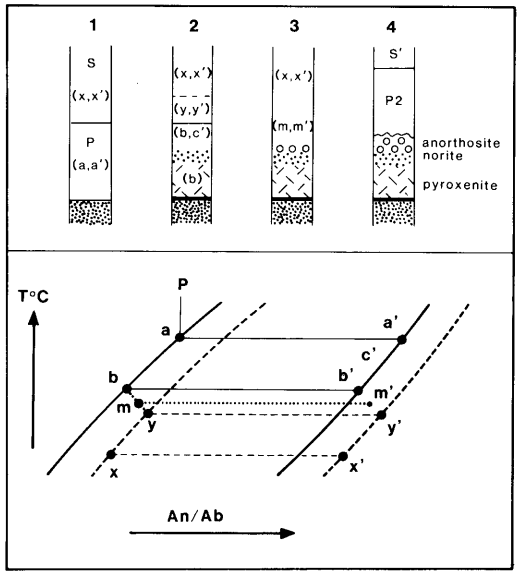

FIG. 9. Schematic representation of plagioclase feldspar relationships during successive stages of development of a cyclic unit, deduced from compositional, textural and Sr-isotope data, and crystal zoning. Solid-line curves depict liquidus and solidus of primitive liquid P, broken-line curves are for liquid residua S of earlier cycles, with higher H_2O content. Bracketed letters in columns above denote compositions in idealized phase diagram below. (1) Newly emplaced, hot, dense, primitive liquid P is emplaced between crystalline floor and column of fractionated residual liquid S, with suspended crystals *x'*. In P, first crystals *a'* are in equilibrium with liquid *a* and crystallize cotectically with ferromagnesian phases. (2) As crystallization of P proceeds and convective turbulence wanes, denser spinel and ferromagnesian silicates collect at base; above this develops a zone of melt *b* enriched in feldspar crystals zoned from *a'* to *b'* (mean composition *c'*). Heating of S above P shifts liquid-crystal equilibrium from *x*–*x'* to *y*–*y'*. (3) On breakdown of diffusive interface between P and S, liquids *b* and *y* mix to yield hybrid *m* with higher An/Ab ratio than *b*. The liquid may then enter the primary phase volume of plagioclase feldspar (see fig. 10) and deposit anorthosite upon norite. Crystals *m'* are more calcic than *b'*, which crystallize from residual melt within intercumulus space of the mafic cumulates. (4) On emplacement of next pulse of primitive liquid P2 the cycle is repeated. Anorthosite floor may undergo partial assimilation to yield characteristic 'dimpled' floor.

Increased Fe/Mg ratios have the same effect. If our assessment of the composition of the supernatant column of residual liquids is correct, progressive mixing with the basal liquid layer would, immediately above the cumulus pyroxenites and norites, shift the liquid composition closer towards feldspar, and expand the primary phase volume of plagioclase (fig. 10). Plagioclase alone would be deposited, yielding an anorthosite layer. Deposition of anorthosite might be transitory, as continued mixing and crystallization would bring the hybrid liquid back towards the orthopyroxene–plagioclase cotectic. A reversion to noritic rock would follow, or a new cycle initiated by a fresh magma input.

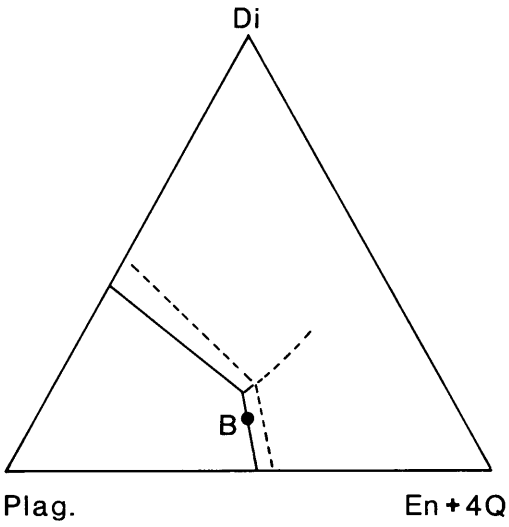

FIG. 10. Schematic representation of relationships within plagioclase–orthopyroxene–clinopyroxene–olivine system, after Irvine (1970, fig. 12). Liquid B on the plagioclase–orthopyroxene cotectic (solid boundary curve) will be within primary phase volume of plagioclase for a higher An/Ab ratio (broken-line boundary curve).

The concept of buoyant plagioclase, and subsequent resorption, cannot be invoked without questioning the composition of the melt itself. Calculations by Irvine *et al.* (1983, p. 1300) show that within the Fo–Di–An–Qz system, melt densities are critically dependent on SiO_2 content. Plagioclase feldspar ($An_{70\ 80}$) is unlikely to float within U-type liquids with the levels of SiO_2 (55–57%) indicated by Sharpe (1985) and Harmer and Sharpe (1985). Light may be shed on the nature of our putative 'primitive liquids' by the studies, by these latter authors, of marginal facies rocks and mafic sills intrusive into the floor of the complex. They define three main groups of quenched rocks, B1, B2, and B3, respectively correlated with the lower zone–lower critical zone, upper critical zone, and main zone lineages. The following features prompt us to link our putative primitive liquids with a picritic facies of the B2 lineage: (*a*) Sr-isotope initial ratios of the B2 lineage are 0.7064–0.7077 (Harmer and Sharpe, 1985, Table 4) matching closely the range (0.7063–0.7080) in the Merensky, Merensky Footwall, and Bastard units (Kruger and Marsh, 1982), (*b*) Zr/Y ratios are within the range 1.0–3.0 in B2 rocks, and close to 2 in our upper critical zone rocks (fig. 6). Corresponding ratios for B1 rocks (5.3–7.4) are much higher, and (*c*) the equation of Roeder and Emslie (1970) or Roeder (1974) indicates that olivine crystallized from B1, B2, and B3 liquids should, respectively, be *c.*Fo_{89-92}, Fo_{75-85}, and Fo_{85-89}. The values indicated for B2 liquids match those recorded (Fo_{76-83}) for the upper critical zone (de Klerk, 1982; Eales and Reynolds, in press) except where olivine–chromite equilibration has occurred. Calculations of this sort are dependent on the convention adopted for assigning Fe^{3+}/Fe^{2+} in whole-rock data, but the argument remains valid even if all Fe in Harmer and Sharpe's analyses is assigned to Fe^{2+}. We conclude therefore that the primitive melts involved in the genesis of the Merensky and Bastard units represent a picritic facies of the SiO_2-poor, basaltic B2 lineage.

The advantages of this reconstruction are (*a*) the proportions of anorthosite within 'complete' cyclic units are not constrained by the initial composition of the freshly emplaced layer of primitive liquid; (*b*) near-total crystallization of such primitive liquids is not necessary, even if such crystallization could end with anorthosite; (*c*) variability in composition of leucocratic rocks is possible; (*d*) progressive changes in isotopic characteristics are possible, if the anorthosites draw part of their substance from the supernatant column, which may in turn be compositionally graded; (*e*) an explanation exists for the anomalously calcic character of many anorthosites, and for intercumulus plagioclase being more sodic than cumulus plagioclase; (*f*) the zonal structure of cumulus plagioclase crystals (cores enclosed by calcic zones, with outer sodic rims) is explained and, by extension, so is rarer oscillatory zoning, in so far as specific feldspar crystals may have survived several cycles before final entrapment in the cumulus assemblage; (*g*) transition within the leucocratic layers to geochemical attributes typical of those within the base of the main zone is explained; (*h*) an explanation for norite–anorthosite–norite sequences is offered; (*i*) the interstitial

habit of pyroxenes within anorthosites is then a consequence of the predicted paragenetic order.

No mechanism for the origin of platinum-group or sulphide mineralization is offered here. Some currently persuasive models rely on an event of catastrophic proportions, such as the mixing of two major columns of liquid (Campbell *et al.*, 1983; Sharpe, 1985) to generate mineralization in the Merensky Reef. As such, the PGE mineralization of the underlying UG2 unit, with an ore reserve twice that of the Merensky unit (Buchanan, 1979), and not insignificant mineralization in the Pseudoreef, are ignored, and deficiencies are thereby revealed in this approach. We comment, however, that Stage 4 of the synthesis presented below is not incompatible with the model of Campbell *et al.* (1983).

Synthesis

The following synthesis postulates a sequence of events that would be consistent with the data available and with the arguments presented. Reconstruction begins with a column of residual, chemically evolved and H_2O-enriched magmatic liquid, with Sr-isotope initial ratio close to 0.7063, above the UG2 pyroxenite (fig. 11, Stage 1). Emplacement of a basal layer of hot, dense, primitive liquid (Stage 2) led to deposition of mafic cumulates with the geochemical affinities (including Sr-isotope ratios) of the underlying rock column. As crystallization proceeded, the liquid density of this layer declined and the diffusive interface with the supernatant liquid column broke down, and mixing was initiated. Leuconorites and anorthosites were deposited while this hybrid liquid was within the primary phase volume of plagioclase, and compatible element and $Sr/Al_2O_3^{\ddagger}$ ratios shifted towards those of the compatible element-depleted supernatant column. This represents the Merensky Footwall unit with its basal harzburgite.

Stage 4 depicts the emplacement of a wedge of main zone liquid some hundreds of metres above the crystalline floor, at a level commensurate with neutral buoyancy within a stratified liquid column. Sr-isotope ratios of this intromittent liquid were *c.*0.709, and Mg/Fe and compatible element ratios consistent with the composition of the Porphyritic Gabbro Marker, crystallized much later. Sr/Al_2O_3 ratios were appropriate to subsequent deposition of feldspars with values in the range $(13–14) \times 10^{-4}$. Progressive mixing is proposed, whereby a column of hybrid liquid was established between the intromittent liquid and the substantive crystalline floor (fig. 11, Stage 5). The column developed a gradation of major- and trace-element, and Sr-isotope ratios, between the present-day top of the Footwall unit and the Porphyritic Gabbro Marker.

Emplacement of a further layer of hot, primitive liquid of the critical zone lineage followed (Stage 6). The resulting mafic cumulates at the base of the Merensky unit reflect the geochemistry of the critical zone lineage. The liquid was initially above the feldspar liquidus, and some resorption of the anorthosite floor was possible, leading to 'dimpling' of that surface. The products of assimilation would have become incorporated within the basal layer, changing its bulk composition and lowering its density. Heat balance requirements would have demanded accelerated deposition of mafic cumulates if assimilation of the floor occurred. As the basal liquid layer crystallized, its density was lowered until mixing with the hybrid layer above was initiated. Compositional attributes (including Sr-isotope ratios) then shifted towards those of the hybrid layer, the liquid entered the primary phase volume of plagioclase *c.*5 atomic % richer in anorthite than in the underlying norites (*see* fig. 10) and highly leucocratic rocks were deposited at the top of the Merensky unit (Stage 7). The results of fractional crystallization of a limited volume of melt were simulated, but the process allowed great variability in the thickness of the anorthosite layer.

The Bastard unit, in principle, repeats the cyclicity of the Merensky unit but displays unique features. Bushveld lore has it that olivine does not occur within the critical zone above the Merensky Reef, but closely spaced sampling by one of us (W.J.deK.) has recently established the presence of several olivine-bearing horizons within the lower part of the unit, separated by olivine-free intervals. This olivine is in places oikocrystic in habit towards robust plagioclase laths; other grains enclose small spheroids of plagioclase resembling remnants of a resorption process. Compositions are $Fo_{78.5}$ to $Fo_{80.5}$ and Ni contents (2800 ppm) are not greatly different to those measured (de Klerk, 1982) in the Merensky Reef (2750–3800 ppm) or Pseudo Reef (2500–3200 ppm) at Union Section. The systematic decline, with stratigraphic height, of Mg/Fe, Co/V, Ni/Sc, and Cr/Sc ratios displayed by the Merensky norites is not as well reproduced in the Bastard unit (fig. 5). Sr-isotope ratios in the Bastard unit extend the trend established in the Merensky unit (fig. 8). Each of these features suggests the crystallization of mafic phases (with critical zone signatures) from a primitive, mafic liquid within which suspended feldspar crystals, derived from the underlying Merensky unit, were trapped while in various stages of assimilation.

The final Stage 9 represents the crystallization of the remainder of the hybrid column as norite, with Sr-isotope ratios rising towards the Porphyritic Gabbro Marker. The saw-tooth pattern of variation in Mg/Fe ratios established by microprobe

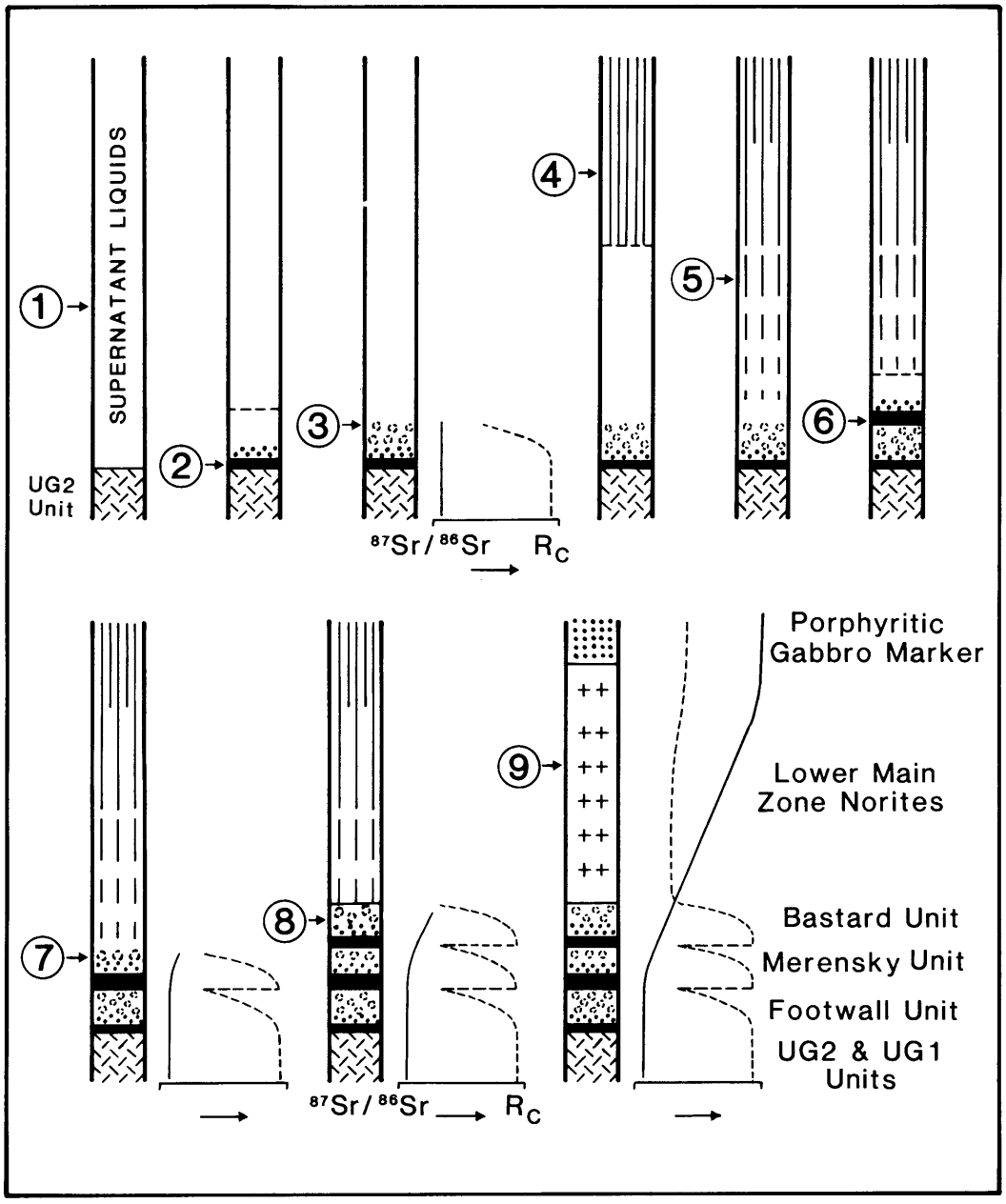

FIG. 11. Schematic outline of development of upper critical zone–lower main zone interval. Stage 2 depicts crystallization of primitive liquid to yield mafic cumulates at base of Merensky Footwall unit; during Stage 3 mixing occurs to yield anorthosites at the top of the unit. Stages 4–5 depict emplacement of main zone liquid and subsequent progressive mixing with older residua to yield gradation in Sr-isotope ratios. Stages 6–7 depict a further injection of primitive liquid of the upper critical zone lineage, and full development of Merensky unit. Development of the Bastard unit (Stage 8) is essentially a repetition of Stage 7. Final stage depicts crystallization of norites, gabbronorites, and Porphyritic Gabbro Marker of main zone. Generalized curves depict $^{87}Sr/^{86}Sr$ ratios, and R_c represents generalized compatible element ratios MgO/(MgO + FeO), Cr/Co, Co/V, and Ni/Sc as shown in fig. 6. Thicknesses of units are not to scale.

analysis of closely spaced samples (Mitchell, 1986) might reflect either crystallization within a stratified liquid, or further, minor episodes of magma injection within this section.

In this paper, we have deliberately avoided discussion of the enigmatic, coarsely pegmatoidal Merensky and Pseudo Reef layers lying at the bases of their respective units. There exist persuasive geochemical, mineralogical and field data that suggest that these specific layers should be regarded as discrete entities whose origin should be sought outside of the framework outlined above.

Acknowledgements. Grateful acknowledgement is made for support under the CSIR National Geoscience Programme. Rustenburg Platinum Mines, Union and Amandelbult Sections, are thanked for logistic support and for allowing free access to their properties. Eugene Cameron is sincerely thanked for allowing H.V.E. to extract analytical data on orthopyroxenes from his extensive files, and Frank Vermaak for graciously making available his profiles through the upper critical zone. Penetrating reviews by Ian Muir and Stephen Sparks were most helpful.

REFERENCES

Buchanan, D. L. (1979) *Univ. Witwatersrand Bureau for Mineral Studies, Report* 4.
Cameron, E. N. (1980) *Econ. Geol.* **75,** 841–71.
——(1982) Ibid. **77,** 1307–27.
Campbell, I. H., Roeder, P. L., and Dixon, J. M. (1978) *Contrib. Mineral. Petrol.* **67,** 369–78.
——Naldrett, A. J., and Barnes, S. J. (1983) *J. Petrol.* **24,** 133–65.
Coetzer, P. M., de Klerk, W. J., and Hatch, N. P. (1981) *Guidebook Third Int. Platinum Symposium, Pretoria,* 20–5.
de Klerk, W. J. (1982) M.Sc. thesis, Rhodes University.
Eales, H. V. In *Guidelines to the evolution of chromite orefields* (C. W. Stowe, ed.). Hutchinson and Ross, Stroudsburg (in press).
——and Marsh, J. S. (1983) *Chem. Geol.* **38,** 57–74.
——and Reynolds, I. M. *Econ. Geol.* (in press).
——Reynolds, I. M., and Gouws, D. A. (1980) *Geol. Soc. S. Africa Trans.* **83,** 243–53.
Gain, S. B. (1985) *Econ. Geol.* **80,** 925–43.
Harmer, R. E., and Sharpe, M. R. (1985) Ibid. **80,** 813–37.
Irvine, T. N. (1970) *Geol. Soc. S. Africa. Spec. Publ.* **1,** 441–76.
——Keith, D. W., and Todd, S. G. (1983) *Econ. Geol.* **78,** 1287–334.
Keith, D. W., Todd, S. G., and Irvine, T. N. (1982) *Carnegie Inst. Washington Yearb.* **81,** 281–94.
Kruger, F. J. (1983) Ph.D. thesis, Rhodes University.
——and Marsh, J. S. (1982) *Nature,* **298,** 53–5.
————(1985) *Econ. Geol.* **80,** 958–74.
——and Mitchell, A. A. (1985) *Can. Mineral.* **23,** 306.
Kushiro, I. (1975) *Am. J. Sci.* **275,** 411–31.
McBirney, A. R., and Noyes, R. M. (1979) *J. Petrol.* **20,** 487–554.
Marsh, J. S., and Eales, H. V. (1984) *Geol. Soc. S. Africa Spec. Publ.* **13,** 27–67.
Mitchell, A. A. (1986) Ph.D. thesis, Rhodes University.
Roeder, P. L. (1974) *Earth Planet. Sci. Lett.* **23,** 397–410.
——and Emslie, R. F. (1970) *Contrib. Mineral. Petrol.* **29,** 275–89.
Scoon, R. N. (1985) Ph.D. thesis, Rhodes University.
Sharpe, M. R. (1985) *Nature,* **316,** 119–26.
Sparks, R. S. J., and Huppert, H. E. (1984) *Contrib. Mineral. Petrol.* **85,** 300–9.
Vermaak, C. F. (1976) *Econ. Geol.* **71,** 1270–98.
von Grunewaldt, G., Sharpe, M. R., and Hatton, C. J. (1985) Ibid. **80,** 803–12.

[*Manuscript received 15 October 1985; revised 24 April 1986*]